Elsevier Editorial System(tm) for Developmental Biology

Manuscript Draft

Manuscript Number: DBIO-09-158

Title: A mortalin-like gene is crucial for planarian stem cell viability

Article Type: Regular Article

Section/Category: Developmental Biology - Main

Keywords: Planarian; Dugesia japonica; Stem cells; Neoblasts; Regeneration; Heat Shock Proteins; HSPs; Mortalin; RNAi; Senescence.

Corresponding Author: Dr Renata Batistoni,

Corresponding Author's Institution: University of Pisa

First Author: Maria Conte, PhD

Order of Authors: Maria Conte, PhD; Paolo Deri, Associate Professor; Maria Emilia Isolani, PhD student; Linda Mannini, Post Doc; Renata Batistoni

Abstract: In adult organisms, stem cells are crucial to homeostasis and regeneration of damage of tissues. In planarians, adult stem cells (neoblasts) are endowed with an extraordinary replicative potential that guarantees unlimited replacement of all differentiated cell types and extraordinary regenerative ability. The molecular mechanisms by which neoblasts combine long-term stability and constant proliferative activity, overcoming the impact of time, remain by far unknown. Here we investigate the role of Djmot, a planarian orthologue that encodes a peculiar member of the HSP70 family, named Mortalin, on the dynamics of stem cells of Dugesia japonica. Planarian stem cells and progenitors constitutively express Djmot. Transient Djmot expression in differentiated tissues is only observed after X-ray irradiation. DjmotRNA interference causes inability to regenerate and death of the animals, as a result of permanent growth arrest of stem cells. These results provide the first evidence that an hsp-related gene is essential for neoblast viability. Here we discuss the

possibility that high levels of Djmot serve to keep a p53-like protein signaling under control, thus allowing neoblasts to escape cell death programs. Further studies are needed to unravel the molecular pathways involved in these processes.

A *mortalin*-like gene is crucial for planarian stem cell viability

Maria Conte, Paolo Deri, Maria Emilia Isolani, Linda Mannini, Renata Batistoni*

Dipartimento di Biologia, Università di Pisa, Italy.

* Corresponding Author: Renata Batistoni, Università di Pisa, Dipartimento di Biologia, Unità di Biologia Cellulare e dello Sviluppo, Via Carducci, 13, I-56017 Ghezzano, Italy

Tel.: +39-050-2211492

fax: +39-050-2211495

e mail: rbatistoni@biologia.unipi.it

Short title: *Djmot* and planarian stem cells

Abstract

In adult organisms, stem cells are crucial to homeostasis and regeneration of damage of tissues. In planarians, adult stem cells (neoblasts) are endowed with an extraordinary replicative potential that guarantees unlimited replacement of all differentiated cell types and extraordinary regenerative ability. The molecular mechanisms by which neoblasts combine long-term stability and constant proliferative activity, overcoming the impact of time, remain by far unknown. Here we investigate the role of *Djmot*, a planarian orthologue that encodes a peculiar member of the HSP70 family, named Mortalin, on the dynamics of stem cells of *Dugesia japonica*. Planarian stem cells and progenitors constitutively express *Djmot*. Transient *Djmot* expression in differentiated tissues is only observed after X-ray irradiation. *Djmot*RNA interference causes inability to regenerate and death of the animals, as a result of permanent growth arrest of stem cells. These results provide the first evidence that an *hsp*-related gene is essential for neoblast viability. Here we discuss the possibility that high levels of *Djmot* serve to keep a p53-like protein signaling under control, thus allowing neoblasts to escape cell death programs. Further studies are needed to unravel the molecular pathways involved in these processes.

keywords: Planarian; *Dugesia japonica*; Stem cells; Neoblasts; Regeneration; Heat Shock Proteins; HSPs; Mortalin; RNAi; Senescence.

Introduction

Adult stem cells maintain homeostasis and regenerate injured tissues over the life span of an individual. The replicative potential of these cells is therefore ultimately responsible for the longevity of multicellular organisms. To prevent senescence and prolong proliferative capacity, stem cells evolved cytoprotective mechanisms to defend themselves against environmental and physiological stresses (Deng, 2008; Ho et al., 2005). However, how these cells adapt to stress in vivo remains largely unknown. In contrast to the limited ability of mammals to renew the missing tissues, some lower organisms show remarkable regenerative power and can rebuild complex body parts, based on the peculiar capability to activate endogenous stem cells and/or dedifferentiate specialized cell types (Sánchez Alvarado and Tsonis, 2006). Planarians (Platyhelminthes) are one of the foremost subjects in regeneration studies. In addition to amazing regenerative abilities, these organisms exhibit high body plasticity and continuous cell turnover throughout life. By constantly renewing the tissues of their body, planarians are thus capable of maintaining a functional body with no evidence of senescence (Pellettieri and Sánchez Alvarado, 2007). These properties are made possible by the presence of neoblasts, a population of somatic cells, that fulfil properties of pluripotent stem cells: i) undergo self-renewing cell divisions, as well as commitment and differentiation into multiple cell types (Handberg-Thorsager et al., 2008), ii) can rescue lethally irradiated worms (Baguñà et al., 1989). Although classically defined as small, undifferentiated cells with a high nucleus/cytoplasm ratio, the recent identification of specific stem cell markers and the ultrastructural analysis of FACS-sorted planarian cells consent now to distinguish neoblast subpopulations, including progenitors and lineage-restricted stem cells (Eisenhoffer et al., 2008; Hayashi et al., 2006; Higuchi et al., 2007; Rossi et al., 2008). These findings reveal that, like mammals, planarian worms possess a complex stem cell system, including progenitors and lineage-restricted stem cells.

Deregulation of protein quality control with consequent accumulation of damaged proteins and an associated functional decline in the protein degradation system represent aging hallmarks in the cell. A remarkable event, which helps to maintain cellular homeostasis under stress, is the production of a highly conserved set of proteins, known as stress or heat shock proteins (HSPs) (Pfanner, 1999; Scheibel and Buchner, 1998). These proteins, broadly classified into different families on the basis of their molecular weight, structure and function, play protective activities involving both the direct maintenance of protein structure as intracellular chaperones and the regulation of death pathways. In addition it is becoming clear that their release into the extracellular microenvironment contributes to the generation of immune response in a number of contexts

(Calderwood et al., 2007; Schmitt et al., 2007). To study the endogenous controls that promote stem cell vitality in the experimentally accessible planarian model is a convenient choice for understanding how growth and aging of adult stem cells are regulated in vivo, rather than after they have changed their properties in culture, and will likely provide insight into the mechanisms that control adult stem cell dynamics in higher organisms. To investigate the potential role of *hsp*-related genes on the dynamics of planarian stem cells, we have begun to identify representative *hsp*-related genes from a planarian EST collection of *Dugesia japonica* (Mineta et al., 2003). Here we report the isolation and functional characterization of a gene (*Djmot*) that encodes an orthologue of a highly conserved, heat-uninducible member of the HSP70 family, also known as Mortalin/GRP75/mthsp70/PBP74 (called Mortalin hereafter) (Kaul et al., 2002). As the diversity of names suggests, this protein is implicated in a variety of functions including cell survival, stress response, intracellular trafficking, control of cell proliferation, mitochondrial biogenesis and cell fate determination (Deocaris et al., 2007; Kaul et al., 2007). Mortalin multifunctional properties correlate with its differential subcellular distributions in normal and immortal cells and with different interactions with multiple partners therein (Deocaris et al., 2007; Wadhwa et al., 2002b). Many cancer and immortal mammalian cells show high levels of *mortalin* expression and its knockdown causes growth arrest (Wadhwa et al., 2004; Wadhwa et al., 2003). Control of cell proliferation has been attributed to a mechanism of Mortalin-dependent cytoplasmic sequestration of p53 tumor suppressor protein, thus preventing its entry in the nucleus (Wadhwa et al., 2002a). Mortalin also plays a critical role in the mechanism that ensures correct centrosome duplication by modulating centrosomal localization of p53 (Ma et al., 2006). Recently it has been reported that the increased expression of the *Caenorhabditis elegans mortalin* orthologue extends the life span of adult worms, while its knockdown causes early aging phenotypes (Kimura et al., 2007; Yokoyama et al., 2002). Mortalin-based cytoplasmic sequestration of a conserved homologue of p53 was also demonstrated in the soft shell clam *Mya arenaria*, a naturally-occurring cancer model (Walker et al., 2006). p53 is cytoplasmically sequestered in clam leukemic hemocytes, but de novo p53 expression, induced by genotoxic stress, can promote its nuclear translocation and cause death of leukemic cells (Bottger et al., 2008). We show that the planarian mortalin-like gene *Djmot* is localized prominently in neoblasts and its functional ablation by RNA interference (RNAi) can permanently arrest the replicative activity and trigger cell death programs in these cells.

Materials And Methods

Animals and treatments

Asexual specimens of *Dugesia japonica* (GI strain) were maintained at 18°C in autoclaved stream water, fed weekly with chicken liver and used for experiments after 10 days of starvation. Thirty days-starved planarians were used for starvation analysis. Regenerating fragments were produced by transverse amputation at prepharyngeal level. Some intact worms were exposed to a lethal dose (30 Gy) of hard X-rays (200 KeV, 1 Gy/min), using a Stabilipan 250/1 instrument (Siemens, Gorla-Siama, Milan, Italy) equipped with a Radiation Monitor 9010 dosimeter (Radcal Corporation, Monrovia, CA, USA). The animals were sacrificed 4, 8, 10, 12 days post-irradiation for subsequent experiments. For heat shock treatment, intact planarians were maintained at 28°C o/n before being harvested for RNA extraction.

Isolation of Djmot

An EST fragment annotated as a homolog of mammalian *mortalin/GRP75* (Mineta et al., 2003) was amplified in *D. japonica* with specific primers. 5'/3' RACE was used to isolate the full-length cDNA (Accession number FM210759).

In situ hybridizations and immunohistochemistry

The riboprobes used in this study were as follows: *Djmot* (1607 to 2039 bp); *Djmcm2* (168 to 761) (Salvetti et al., 2000); *Djnos* (85 to 585 bp) (Sato et al., 2006); *DjPiwi-1* (1911 to 2379 bp) (Rossi et al., 2006). All digoxigenin-labelled riboprobes were prepared using digoxigenin-labelling kit (Roche), according to the manufacturer's instructions. Whole mount in situ hybridization was performed in intact and regenerating animals according to Umesono et al., (Umesono et al., 1997) with minor modifications (Nogi and Levin, 2005). To prepare sections, animals were fixed in cold relaxant solution (Kobayashi et al., 1998). In situ hybridization on paraffin-embedded sections (6 μm thickness) was performed as described by Kobayashi et al. (1998). The sections were then stained immunohistochemically with DjPCNA primary antibody (1:800) (Ito et al., 2001; Orii et al., 2005). After washing, goat anti-rabbit conjugated to Alexa 488 (Molecular Probes) as a secondary antibody, diluted 1:1000. Immunohistochemistry on dissociated cells (Baguñà and Romero, 1981; Salvetti et al., 2000) was performed using a polyclonal antibody raised against a 21-residue peptide

corresponding to the p53-binding domain of *M. arenaria* Mortalin (Mamot) (1:25) (Walker et al., 2006) and visualized with goat anti-rabbit (1:1000) conjugated to Alexa 488 (Molecular Probes) secondary antibody. The specificity of Mamot primary antibody to planarians was assayed by Western blot analysis. Western blot was performed basically as described by Orii et al., (2005). After electrophoretic transfer, the membrane was incubated with anti-Mamot antibody, diluted 1:1000. After incubation with 1:10,000 dilution of anti-rabbit Perossidase secondary antibody (Sigma), detection was performed using Lumi-Light Western blotting Substrate reagents (Roche).

Real Time RT-PCR

Total RNA was extracted with the NucleoSpin RNAII kit (Macherey-Nagel). Each extraction was tested for the absence of genomic DNA by control RT-PCR reactions performed in the absence of reverse transcriptase. cDNA was generated from DNaseI-treated total RNA using Superscript First Strand Synthesis System (Invitrogen). Each cDNA samples was obtained from three intact or regenerating planarians. Real time RT-PCR was performed at least three times with independent RNA samples. Specific sense and antisense oligonucleotides (Supplementary Table I) were generated using LaunchNetPrimer software. SYBR Green chemistry-based RT-PCR was carried out on a Rotor-Gene 6000 Real time-PCR (Corbett Research). After an initial denaturation step (5 min at 95°C), 45 cycles of amplification were performed as follows: denaturation: 95°C, 15s, annealing: 60°C, 20s, extension: 72°C, 40s. Melt analysis was performed at the end of the run using the RotorGene software.

RNA interference

Double-stranded RNA (dsRNA) was synthesized according to Sánchez Alvarado and Newmark (1999). dsRNA was obtained from *Djmot* (1607 to 2039 bp) and the injection schedule was as described by Mannini et al. (Mannini et al., 2004). All amputated fragments were analyzed during the second round of regeneration. Intact animals were analyzed after 20 days from the first injection. The reduction of the endogenous transcripts after RNAi was assessed by real time RT-PCR. For mitotic index analysis, both intact planarians and fragments regenerating a head or a tail of *Djmot* dsRNA-injected planarians and water-injected controls were incubated for 6 hours in 3‰ colchicine (w/v) (Sigma) and sacrificed 10 or 20 days. The animals were dissociated into single cells (Baguñà and Romero, 1981) and 20µl of the cell suspension was dropped onto glass slides, air-dried and stained with a 1µg/mL Hoechst 33342. The number of mitotic metaphases was monitored under a

fluorescence microscope. Three specimens were analyzed for each time; two slides for each sample were examined for a total of about 80,000 cells. The number of cells contained in the 20µl aliquot was counted by using a hemocytometer.

Results

Characterization of a mortalin-*like gene in planarians*

A cDNA sequence (*Djmot*) with significant similarity to mammalian *mortalin* genes was identified in *D. japonica*. The predicted DjMot protein (680 amino acids) shows an amino-terminal presequence, a HSP70 motif with an ATPase domain and a peptide binding domain. Moreover, the p53-binding sequence, mapped in the ATPase domain of Mortalin (Kaul et al., 2001) appears well conserved in DjMot (amino acids 295-315) (Fig. 1A,B). Literature data demonstrate that Mortalin may sequester the tumor suppressor protein p53 in the cytoplasm, preventing its nuclear translocation (Kaul et al., 2005; Wadhwa et al., 2002a; Walker et al., 2006). As the sequence of p53-binding domain of DjMot and the corresponding domain of *M. arenaria* Mortalin differ only for three aminoacids (*M. arenaria*: CRLREAAEKAKIELSSSLQTD; *D. japonica*: QRVREAAEKAKIELSSALQTD), we used a polyclonal antibody raised against this specific region in *M. arenaria* (Mamot: Walker et al., 2006) to perform immunohistochemistry on planarian dissociated cells. The results, also confirmed by Western blot analysis (not shown), demonstrated Mamot cross-reaction in small neoblast-like cells (Fig. 1C). Although as indirect evidence, this finding supports the possibility of an evolutionary conserved role for DjMot in sequestering a p53-like protein in the cytoplasm.

Whole mount in situ hybridization on intact and regenerating planarians provided a spatial analysis of *Djmot* expression. In intact animals, staining was observed in the mesenchymal tissue (parenchyma) (Fig. 2A), with a pattern that reflects the distribution of neoblasts (Rossi et al., 2008). Because parenchymal tissue contains a number of different cell types, in situ hybridization was also performed on sections (Fig. 2B,C). *Djmot* transcripts could be visualized in small neoblast-like cells (Fig. 2D). Double staining of *Djmot* mRNA and the neoblast-specific DjPCNA antibody (Fig. 2E) (Orii et al., 2005) revealed that DjPCNA-positive cells were also *Djmot*-positive (Fig. 2B,C,F). However, we observed that some *Djmot*-positive neoblast-like cells were DjPCNA-negative. In regenerating animals, strong *Djmot* expression was observed in the postblastema (Fig. 2G,H), the stump region beneath the wound comprised of actively proliferating neoblasts (Salvetti et al., 2000). *Djmot* expression, however, was also detected in the early blastemal tissue, a postmitotic area where

neoblast progeny undergoes differentiation (Fig. 2G,H). Such expression decreased as regeneration proceeded (not shown), suggesting that residual *Djmot* transcripts can be found in postmitotic progeny.

Implication of Djmot *in the radio-adaptive response*

As *Djmot* expression appears associated to neoblasts, we selectively killed them by a lethal dose (30 Gy) of X-ray irradiation (Hayashi et al., 2006; Reddien et al., 2005; Rossi et al., 2008; Salvetti et al., 2000) and then evaluated the effects at different times from the treatment. At 4 days after irradiation the parenchymal expression of *Djmot* appeared strongly reduced. At the same time, a new expression profile was detected with respect to untreated controls, because specific *Djmot* transcripts could be observed at the gastrodermal level. *Djmot* expression in the gastrodermis then declined at an undetectable level. Remarkably, after 8 days the level of *Djmot* mRNA became consistently elevated in the central nervous system. Finally, at 10 days after irradiation, no *Djmot* expression could be detected (Fig. 3A-C). To further assess how the level of *Djmot* RNA could be modulated by different stress conditions, some planarians were sacrificed after a long period of starvation or exposed to heat shock. Starved planarians maintained an unaltered expression pattern, but a 3-fold increase in *Djmot* expression level was observed relative to controls (Fig. 3D,E), indicating that DjMot also plays a role in regulating body size according to the metabolic status. *Djmot* RNA level did not increase in heat-shocked animals, providing evidence that DjMot is a heat-uninducible member of the HSP70 family (Fig. 3F).

Effects of Djmot*RNAi on intact and regenerating planarians*

To assess the role of *Djmot* on neoblast biology we performed RNAi experiments (Sánchez Alvarado and Newmark, 1999) and evaluated the effects on intact animals and during regeneration. A significant reduction in endogenous *Djmot* RNA level was observed in injected specimens with respect to water-injected controls (Supplementary Fig. 1A-C). The levels of *Djhsp60* (Rossi et al., 2007) and *Djhsc70*, (a gene coding for the constitutive HSP70 form of *D. japonica*) were not affected, indicating that the *Djmot*RNAi effect was specific (data not shown). We observed that *Djmot*RNAi strongly inhibited blastema formation. Most of the injected fragments (153/170) completely failed to regenerate new tails, and the wound region often appeared indented (Fig. 4A-C), while 10% partially regenerated. The penetrance of tail fragments completely unable to regenerate a new head was 80% (136/170), while regeneration of a small head could be observed in

20% (34/170) of the phenotypes. These small heads also showed an abnormal morphogenesis (Fig. 4D-F), as visualized by the use of the eye specific marker, *Djops* (Mannini et al., 2004) (Fig. 4G-I). Furthermore, *Djmot*RNAi injected animals showed gradual head regression and/or lysis and died in 5-7 weeks from the beginning of the treatment, while the survival of controls was not affected. These results suggest that *Djmot* is critical for neoblast activity during regeneration and tissue homeostasis. We further explored the possibility that the functional ablation of this gene had an effect on cell divisions by monitoring the percentage of mitoses in *Djmot*RNAi animals compared to controls. We observed that *Djmot*RNAi caused a dramatic reduction in the number of mitotic cells both in intact animals and amputated fragments (Fig. 4L,M).

Screen for molecular markers in Djmot*RNAi planarians*

In accordance with the finding that *Djmot*RNAi affects the mitotic activity of neoblasts, we observed a severe reduction in the expression level of the proliferation-related marker *Djmcm2* (Salvetti et al., 2000) in injected animals (Fig. 5A-C). To evaluate whether *Djmot* knockdown affected differently the neoblast subpopulations identified in planarians, we characterized the expression of *Djnos*, a *nanos*-related gene specifically found in germline stem cells (Handberg-Thorsager and Saló, 2007; Sato et al., 2006; Wang et al., 2007), and of *DjPiwi-1*, a homologue of *Drosophila Piwi* (Cox et al., 1998), preferentially localized in stem cells of the dorsal midline (Rossi et al., 2006). *Djnos* expression dramatically decreased in *Djmot*RNAi animals when compared to controls (Fig. 6A-C). A different situation was observed using *DjPiwi-1* (Fig. 7A-E). *DjPiwi-1* expression level showed only a slight decrease after *Djmot*RNAi (Fig. 7A,C). In addition we noted that *Djmot*RNAi caused modification in *DjPiwi-1* expression pattern in some injected animals. Two parallel rows of hybridization signal could be in fact detected near the posterior region of the brain (Fig. 7E). This pattern was never observed in control animals, that showed *DjPiwi-1*-positive cells only at the midline level (Fig. 7B,D).

As *Djmot*-expression was detected both in neoblasts and postmitotic descendants, we also investigated *Djinx-11*, a stem cell gap junction gene, whose expression may reflect the transition state from neoblasts to differentiating progeny (Gurley and Sánchez Alvarado, 2008; Nogi and Levin, 2005). Our data clearly demonstrate that *Djinx-11* is strongly reduced after *Djmot*RNAi (Fig. 8A). On the contrary, *Djmot*RNAi did not interfere with the expression of *DjSyt* (Tazaki et al., 1999) and *Djmhc-B* (Kobayashi et al., 1998), that are specific markers for nerve and muscle cells, respectively (Fig. 8B,C). These findings indicate that, lacking the function of *Djmot*, both planarian

stem cells and their progeny do not survive much longer, while *Djmot* knockdown produce no or limited effects on differentiated cells.

Discussion

Expression profile of Djmot

Planarians provide a unique experimental model for studying in vivo the molecules and processes that consent to these cells to combine long-term stability and constant proliferative activity, overcoming the impact of time without escaping normal regulatory control and generating tumors or aging. The molecular events that allow neoblasts to escape cellular senescence remain undefined so far. In this study we describe a planarian *hsp70*-related gene, *Djmot*, capable of regulating stem cell growth. High levels of *Djmot* transcripts were seen as being confined to proliferating neoblasts and their descendants, while no detectable expression could be found in differentiated cells of intact and regenerating planarians. Immunolocalization in dissociated cells also confirmed the presence of high levels of DjMot protein only in neoblast-like cells. As X-ray treatment causes rapid and selective death of neoblasts, we also compared the expression profile of *Djmot* before and after irradiation and observed that the parenchymal expression of *Djmot* became dramatically downregulated in irradiated worms. However, irradiation also elicited transient induction of *Djmot* expression in intestine and nerve cells, suggesting that, under stress conditions, this gene is involved in activating compensatory mechanisms, e.g. unfolded protein response (UPR), to prolong the life of differentiated cells (Kim, 2008). These observations indicate that planarians may activate efficient mechanisms to reduce the effects of stress stimuli in compromised tissues, although this was not by itself sufficient to ensure planarian survival after X-ray treatment, because no stem cells were further available to sustain normal tissue replacement.

Djmot *knockdown results in an inability of planarians to maintain vital neoblasts*

The phenotypes associated with *Djmot*RNAi implicate an essential role for this gene in maintaining vital neoblasts. Inability to regenerate and successive death of the animals, as well as dramatic decline of proliferative capacity, were in fact observed as a consequence of *Djmot* knockdown. We asked whether *Djmot* was necessary to prevent growth arrest in cycling stem cells of planarians. To support this possibility, a variable number of cells showing a senescence-associated morphology,

i.e. flattened, enlarged cells with condensed chromatin, could be detected in dissociated cells of *Djmot*RNAi planarians (Fig. 9A-D). This type of cells was never observed in control animals. Unfortunately, no biomarkers for visualization and quantification of senescent cells are available for planarians. Moreover, in our hands TUNEL assay (Hwang et al., 2004) did not work well and did not provide clear evidence of the presence of apoptotic cells. We suggest that the relationship between the functional ablation of *Djmot* and accumulation of senescent cells could be related to conserved ability of Mortalin proteins to sequester the tumor suppressor protein p53 in the cytoplasm, thus promoting lifespan and cellular immortalization (Wadhwa et al., 2002a; Wadhwa et al., 1998; Walker et al., 2006). Our immunostaining data using Mamot – an antibody raised against the p53 binding sequence of *M. arenaria* (Walker et al., 2006), and conserved in DjMot – demonstrate cross-reaction in neoblast cells, supporting the possibility that DjMot binds the cytoplasmic sequestration domain of a yet unknown planarian p53-like protein. Silencing *Djmot* by RNAi could prevent formation of the Mortalin-p53 complex, allowing p53 to enter the nucleus. As overexpression of p53 leads to permanent cell cycle arrest or apoptosis in other organisms, we are tempting to speculate that compromising this mechanism we permanently halt the cell division cycle in neoblasts, inducing a senescent state (Fig. 9A-D). Further studies, including characterization of *p53*-related genes in planarians, are needed to confirm this possibility and elucidate the molecular pathways implicated in growth control of planarian stem cells.

Djmot *and dynamics of neoblast subpopulations*

Both in situ and real time RT PCR analyses with specific markers allowed us to evaluate the relevance of *Djmot* function in different subpopulations of planarian stem cells. A general reduction in the expression level of all analyzed neoblast markers was observed as a consequence of the functional ablation of *Djmot*, with the exception of *DjPiwi-1*. We believe that the partial reduction of *DjPiwi-1* mRNA level may depend on the heterogeneous composition of *DjPiwi-1*-positive cells (Rossi et al., 2006). Probably only a part of *DjPiwi-1*-positive cells express *Djmot* and therefore are sensible to *Djmot*RNAi. More difficult is to find an explanation for the variation in the expression pattern of *DjPiwi-1* in *Djmot*RNAi animals. Bearing in mind that the posterior region of the brain expresses the *wnt* homolog *DjwntA* (Kobayashi, 2007), we can only speculate that the variation of *DjPiwi-1* pattern is in some way related to Wnt signaling on *DjPiwi-1* positive/*Djmot* negative cells, a possibility that deserves further investigation.

Interestingly, lineage-restricted stem cells, such as those identified by the expression of the planarian *nanos* homolog *Djnos* (Sato et al., 2006) in the presumptive ovary or testis-forming

regions, were also affected by *Djmot*RNAi. These cells are DjPCNA positive and BrdU negative cells, and have been considered in a transient state of cell cycle arrest in asexual planarians (Rossi et al., 2008; Sato et al., 2006). We believe that they constitute a short-lived X ray-sensitive progeny, constantly replaced by the proliferative action of cycling neoblasts, sensitive to *Djmot* function (Wang et al., 2007). Furthermore, *Djinx-11*, a neoblast-specific gap junction gene, whose expression probably reflects the transition state from neoblasts to differentiating progeny (Gurley and Sánchez Alvarado, 2008), became strongly downregulated after *Djmot*RNAi. On the contrary, markers of differentiated cell types appeared to be insensitive to functional inactivation of this gene. Taken together, our findings indicate DjMot as an essential component of the regulatory machinery that maintains neoblasts in a mitotically active condition to constantly supply progenitors, and, in turn, sustain the physiological turnover of all differentiated cells. Loss of neoblast progeny after *Djmot*RNAi might be only an indirect effect of a permanent growth arrest of stem cells. Further studies are needed for elucidate the precise mechanism of action of this gene and how such control is lifted by its loss.

Acknowledgments

We are indebted to Dr. H. Orii and Dr. S. Böttger for provide us with aliquots of PCNA antibody and Mamot antibody, respectively. We also thank Dr. C. Pugliesi for X-ray irradiation. This research was supported by grants from Pisa University, Italy.

References

Baguñà, J. and Romero, R. (1981). Quantitative analysis of cell types during growth, degrowth ane regeneration in the planarians *Dugesia mediterranea* and *Dugesia tigrina*. Hydrobiologia 84, 181-194 Scopus.

Baguñà, J., Saló, E. and Auladell, C. (1989). Regeneration and pattern formation in planarians. III. Evidence that neoblasts are totipotent stem cells and the source of blastema cells. Development 107, 77-86 Scopus.

Bottger, S., Jerszyk, E., Low, B. and Walker, C. (2008). Genotoxic stress-induced expression of p53 and apoptosis in leukemic clam hemocytes with cytoplasmically sequestered p53. Cancer Res 68, 777-82 Scopus.

Calderwood, S. K., Mambula, S. S. and Gray, P. J., Jr. (2007). Extracellular heat shock proteins in cell signaling and immunity. Ann N Y Acad Sci 1113, 28-39 Scopus.

Cox, D. N., Chao, A., Baker, J., Chang, L., Qiao, D. and Lin, H. (1998). A novel class of evolutionarily conserved genes defined by piwi are essential for stem cell self-renewal. Genes Dev 12, 3715-27 Scopus.

Deng, Y., Chan, S. S., Chang S. (2008). Telomere dysfunction and tumor suppression: the senescence connection. Nat Rev Cancer, 450-458.

Deocaris, C. C., Widodo, N., Ishii, T., Kaul, S. C. and Wadhwa, R. (2007). Functional significance of minor structural and expression changes in stress chaperone mortalin. Ann N Y Acad Sci 1119, 165-75 Scopus.

Eisenhoffer, G. T., Kang, H. and Alvarado, A. S. (2008). Molecular analysis of stem cells and their descendants during cell turnover and regeneration in the planarian Schmidtea mediterranea. Cell Stem Cell 3, 327-39 Scopus.

Gurley, K. A. and Sánchez Alvarado, A. (2008). Stem cells in animal models of regeneration. StemBook, ed. The Stem Cell Research Community, 1-23.

Handberg-Thorsager, M., Fernandez, E. and Saló, E. (2008). Stem cells and regeneration in planarians. Front Biosci 13, 6374-94 Scopus.

Handberg-Thorsager, M. and Saló, E. (2007). The planarian nanos-like gene Smednos is expressed in germline and eye precursor cells during development and regeneration. Dev Genes Evol 217, 403-11 Scopus.

Hayashi, T., Asami, M., Higuchi, S., Shibata, N. and Agata, K. (2006). Isolation of planarian X-ray-sensitive stem cells by fluorescence-activated cell sorting. *Dev* Growth Differ 48, 371-80 Scopus.

Higuchi, S., Hayashi, T., Hori, I., Shibata, N., Sakamoto, H. and Agata, K. (2007). Characterization and categorization of fluorescence activated cell sorted planarian stem cells by ultrastructural analysis. Dev Growth Differ 49, 571-81 Scopus.

Ho, A. D., Wagner, W. and Mahlknecht, U. (2005). Stem cells and ageing. The potential of stem cells to overcome age-related deteriorations of the body in regenerative medicine. EMBO Rep 6 Spec No, S35-8.

Hwang, J. S., Kobayashi, C., Agata, K., Ikeo, K. and Gojobori, T. (2004). Detection of apoptosis during planarian regeneration by the expression of apoptosis-related genes and TUNEL assay. Gene 333, 15-25 Scopus.

Ito, H., Saito, Y., Watanabe, K. and Orii, H. (2001). Epimorphic regeneration of the distal part of the planarian pharynx. . Dev Genes Evol 211, 2-9 Scopus.

Kaul, S. C., Aida, S., Yaguchi, T., Kaur, K. and Wadhwa, R. (2005). Activation of wild type p53 function by its mortalin-binding, cytoplasmically localizing carboxyl terminus peptides. J Biol Chem 280, 39373-9 Scopus.

Kaul, S. C., Deocaris, C. C. and Wadhwa, R. (2007). Three faces of mortalin: a housekeeper, guardian and killer. Exp Gerontol 42, 263-74 Scopus.

Kaul, S. C., Reddel, R. R., Mitsui, Y. and Wadhwa, R. (2001). An N-terminal region of mot-2 binds to p53 in vitro. Neoplasia 3, 110-4.

Kaul, S. C., Taira, K., Pereira-Smith, O. M. and Wadhwa, R. (2002). Mortalin: present and prospective. Exp Gerontol 37, 1157-64 Scopus.

Kim, I., Xu, W., Reed, J. C. (2008). Cell death and endoplasmic reticulum stress disease relevance and therapeutic opportunities. Nat Rev Drug Discov 7, 1013-1030 Scopus.

Kimura, K., Tanaka, N., Nakamura, N., Takano, S. and Ohkuma, S. (2007). Knockdown of mitochondrial heat shock protein 70 promotes progeria-like phenotypes in caenorhabditis elegans. J Biol Chem 282, 5910-8 Scopus.

Kobayashi, C., Kobayashi, S., Orii, H., Watanabe, K. and Agata, K. (1998). Identification of Two Distinct Muscles in the Planarian *Dugesia japonica* by their Expression of Myosin Heavy Chain Genes. Zoolog Sci 15, 861-869 Scopus.

Kobayashi, C., Saito, Y., Ogawa, K., Agata, K. (2007). Wnt signaling is required for antero-posterior patterning of the planarian brain. Dev Biol.

Ma, Z., Izumi, H., Kanai, M., Kabuyama, Y., Ahn, N. G. and Fukasawa, K. (2006). Mortalin controls centrosome duplication via modulating centrosomal localization of p53. Oncogene 25, 5377-90 Scopus.

Mannini, L., Rossi, L., Deri, P., Gremigni, V., Salvetti, A., Salo, E. and Batistoni, R. (2004). Djeyes absent (Djeya) controls prototypic planarian eye regeneration by cooperating with the transcription factor Djsix-1. Dev Biol 269, 346-59 Scopus.

Mineta, K., Nakazawa, M., Cebria, F., Ikeo, K., Agata, K. and Gojobori, T. (2003). Origin and evolutionary process of the CNS elucidated by comparative genomics analysis of planarian ESTs. Proc Natl Acad Sci U S A 100, 7666-71 Scopus.

Nogi, T. and Levin, M. (2005). Characterization of innexin gene expression and functional roles of gap-junctional communication in planarian regeneration. Dev Biol 287, 314-35 Scopus.

Orii, H., Sakurai, T. and Watanabe, K. (2005). Distribution of the stem cells (neoblasts) in the planarian *Dugesia japonica*. Dev Genes Evol 215, 143-157 Scopus.

Pellettieri, J. and Sánchez Alvarado, A. (2007). Cell turnover and adult tissue homeostasis: from humans to planarians. Annu Rev Genet 41, 83-105 Scopus.

Pfanner, N. (1999). Who chaperones nascent chains in bacteria? Curr Biol 9, R720-4.

Reddien, P. W., Bermange, A. L., Murfitt, K. J., Jennings, J. R. and Sánchez Alvarado, A. (2005). Identification of genes needed for regeneration, stem cell function, and tissue homeostasis by systematic gene perturbation in planaria. Dev Cell 8, 635-49 Scopus.

Rossi, L., Salvetti, A., Batistoni, R., Deri, P. and Gremigni, V. (2008). Planarians, a tale of stem cells. Cell Mol Life Sci 65, 16-23.

Rossi, L., Salvetti, A., Lena, A., Batistoni, R., Deri, P., Pugliesi, C., Loreti, E. and Gremigni, V. (2006). *DjPiwi-1*, a member of the PAZ-Piwi gene family, defines a subpopulation of planarian stem cells. Dev Genes Evol 216, 335-346 Scopus.

Rossi, L., Salvetti, A., Marincola, F. M., Lena, A., Deri, P., Mannini, L., Batistoni, R., Wang, E. and Gremigni, V. (2007). Deciphering the molecular machinery of stem cells: a look at the neoblast gene expression profile. Genome Biol 8, R62.

Salvetti, A., Rossi, L., Deri, P. and Batistoni, R. (2000). An MCM2-related gene is expressed in proliferating cells of intact and regenerating planarians. Dev Dyn 218, 603-14 Scopus.

Sánchez Alvarado, A. and Newmark, P. A. (1999). Double-stranded RNA specifically disrupts gene expression during planarian regeneration. Proc Natl Acad Sci U S A 96, 5049-54 Scopus.

Sánchez Alvarado, A. and Tsonis, P. A. (2006). Bridging the regeneration gap: genetic insights from diverse animal models. Nat Rev Genet 7, 873-84 Scopus.

Sato, K., Shibata, N., Orii, H., Amikura, R., Sakurai, T., Agata, K., Kobayashi, S. and Watanabe, K. (2006). Identification and origin of the germline stem cells as revealed by the expression of nanos-related gene in planarians. Dev Growth Differ 48, 615-28 Scopus.

Scheibel, T. and Buchner, J. (1998). The Hsp90 complex--a super-chaperone machine as a novel drug target. Biochem Pharmacol 56, 675-82 Scopus.

Schmitt, E., Gehrmann, M., Brunet, M., Multhoff, G. and Garrido, C. (2007). Intracellular and extracellular functions of heat shock proteins: repercussions in cancer therapy. J Leukoc Biol 81, 15-27 Scopus.

Tazaki, A., Gaudieri, S., Ikeo, K., Gojobori, T., Watanabe, K. and Agata, K. (1999). Neural network in planarian revealed by an antibody against planarian synaptotagmin homologue. Biochem Biophys Res Commun 260, 426-32 Scopus.

Umesono, Y., Watanabe, K. and Agata, K. (1997). A planarian orthopedia homolog is specifically expressed in the branch region of both the mature and regenerating brain. Dev Growth Differ 39, 723-7 Scopus.

Wadhwa, R., Taira, K. and Kaul, S. C. (2002a). An Hsp70 family chaperone, mortalin/mthsp70/PBP74/Grp75: what, when, and where? Cell Stress Chaperones 7, 309-16.

Wadhwa, R., Takano, S., Robert, M., Yoshida, A., Nomura, H., Reddel, R. R., Mitsui, Y. and Kaul, S. C. (1998). Inactivation of tumor suppressor p53 by mot-2, a hsp70 family member. J Biol Chem 273, 29586-29591.

Wadhwa, R., Takano, S., Taira, K. and Kaul, S. C. (2004). Reduction in mortalin level by its antisense expression causes senescence-like growth arrest in human immortalized cells. J Gene Med 6, 439-44 Scopus.

Wadhwa, R., Yaguchi, T., Hasan, M. K., Mitsui, Y., Reddel, R. R. and Kaul, S. C. (2002b). Hsp70 family member, mot-2/mthsp70/GRP75, binds to the cytoplasmic sequestration domain of the p53 protein. Exp Cell Res 274, 246-53 Scopus.

Wadhwa, R., Yaguchi, T., Hasan, M. K., Taira, K. and Kaul, S. C. (2003). Mortalin-MPD (mevalonate pyrophosphate decarboxylase) interactions and their role in control of cellular proliferation. Biochem Biophys Res Commun 302, 735-42 Scopus.

Walker, C., Bottger, S. and Low, B. (2006). Mortalin-based cytoplasmic sequestration of p53 in a nonmammalian cancer model. Am J Pathol 168, 1526-30 Scopus.

Wang, Y., Zayas, R. M., Guo, T. and Newmark, P. A. (2007). nanos function is essential for development and regeneration of planarian germ cells. Proc Natl Acad Sci U S A 104, 5901-6 Scopus.

Yokoyama, K., Fukumoto, K. and Murakami, T. (2002). Extended longevity of Caenorhabditis elegans by knocking in extra copies of hsp70F, a homolog of mot-2 (mortalin/mthhsp70/Grp75). FEBS Lett 516, 53-57 Scopus.

Figure Legends

Fig. 1

Djmot is a predicted orthologue of mammalian Mortalin. **A)** Schematic representation of Djmot protein and **B)** amino acid sequence deduced from the open reading frame of *Djmot* cDNA. Like other members of the Hsp70 family, Djmot is composed of two highly conserved regions: an amino-terminal ATPase domain (orange: amino acid 45-422) and a peptide binding domain (purple: amino acid 423-649). The sequence showing high similarity with the p53 binding region of *Mya arenaria* mortalin is underlined in green. The major differences with Mortalin proteins of other organisms are found in the first 44 residues of the N-terminal region (blue: presequence; the conserved mitocondrial localization signal IRLYS is underlined in red), and in the carboxy-terminal segment (yellow). In particular the C-terminal domain does not contain the conserved PTIEEVD motif, found in the constitutive form of HSP70 identified in *D. japonica* (DjHSC70: accession number ABY83101). **C)** Mamot antibody immunostaining on a dissociated neoblast-like cell **a)** Phase contrast image; **b)** Nucleus staining with ethidium homodimer (red). **c)** Expression of Mamot antibody (green). **d)** Merge of figures (c) and (d**)**. Scale bar 10 μm.

Fig. 2

Analysis of *Djmot* expression in *D. japonica*. A) Whole mount *in situ* hybridization in an intact planarian. **B)** Schematic of the figure depicted in (C) (ep: epidermis; g: gut). **C)** *In situ* hybridization and DjPCNA antibody immunostaining on a transverse wax section: *Djmot* expression in purple and DjPCNA immunolocalization in green. **D)** Enlarged view of a neoblast-like cell expressing *Djmot* mRNA. **E)** The same cell after DjPCNA antibody immunostaining. **F)** Merge of D and E. **G)** Schematic of a planarian regenerating a head (bl: blastema). The region depicted in H is boxed. **H)** *Djmot* expression during head regeneration (2 days after amputation). The dashed yellow line indicates the border between the regenerating area and the stump. Anterior is on the top. Scale bars: 500 μm in A, 20 μm in C, 10 μm in D-F, 50 μm in H.

Fig. 3

***Djmot* expression in different stress conditions**. **A-C)** Whole mount *in situ* hybridization analysis after X-ray irradiation (30Gy). **A**) 4d: 4 days after irradiation, **B**) 8d: 8 days after irradiation, **C**) 10d: 10 days after irradiation. **D,E)** *Djmot* expression analysis after starvation (30 days). **D**) Whole mount *in situ* hybrididazion. **E**) Real time RT-PCR. C: control, S: starved animals. Each value is the mean ± s.d. of three independent samples, analysed in triplicate. Samples were compared using the

unpaired t-test.**P<0.001. **F)** Real time RT-PCR after heat shock (28°C for 20 hours) (C: control, HS heat shocked animals). Expression levels in E and F are indicated in relative units assuming as unitary the value of untreated specimens. Scale bars: 500 μm in A-C, 200 μm in D.

Fig. 4

Analysis of *Djmot*RNAi phenotypes. A) Schematic of regenerating planarian fragments. bl: blastema. **B,C)** Bright-field images of head fragments, 20 days after amputation. **B)** A water-injected control regenerating a tail. The dashed yellow line indicates the border between the regenerating area and the stump. **C)** A *Djmot*RNAi phenotype. The wound region appears indented and does not form blastema (arrow). **D-F)** Bright-field images of tail fragments, 20 days after amputation. **D)** Visualization of a regenerated head of a water-injected control. **E)** A small, abnormal head is regenerated after *Djmot* RNAi. **F**) A phenotype unable to regenerate after *Djmot* RNAi. The dashed yellow line indicates the border between the regenerating area and the stump. Anterior is on the top. **G-I)** Whole mount *in situ* hybridization with *Djops* of the planarian fragments depicted in D-F. **G)** *Djops* hybridization signal is clearly detected at the eye level in the water-injected control. **H)** *Djops* expression is detected in the small cyclopic eye of the small, abnormal head regenerated after *Djmot* RNAi. **I)** No *Djops* hybridization signal can be detected in the phenotype unable to regenerate after *Djmot* RNAi. **L)** Analysis of the percentage of mitoses in intact animals (dark gray) and **M**) during regeneration (light gray), (c: control). The number of mitotic metaphases was normalized to the number of total cells and the values indicated in the graphs are average ± s. d. of three independent samples. Samples were compared using the unpaired *t*-test. **P<0.001, ***P<0.0001. Scale bar 500 μm in B,C and 40μm in D-I.

Fig. 5:

Expression of *Djmcm2* after *Djmot* RNAi. A) Expression level analyzed by real time RT-PCR in water-injected controls (c) and in *Djmot* RNAi animals. **B)** Expression in a regenerating head of a water-injected control. **C)** Expression in a tail fragment unable to regenerate after *Djmot*RNAi. Expression analyses were performed on fragments 20 days after amputation. In the real time RT-PCR experiment the expression level is indicated in relative units, assuming as unitary the value of the control. Samples were compared using the un-paired t-test. **P<0.001. The dashed yellow lines indicate the border between the regenerating area and the stump. Anterior is on the top. Scale bar 200 μm.

Fig.6:

Expression of *Djnos* after *Djmot* RNAi. A) Expression level analyzed by real time RT-PCR in water-injected controls (c) and in *Djmot* RNAi animals. **B)** Expression in a regenerating head of a water-injected control. **C)** Expression in a tail fragment unable to regenerate after *Djmot*RNAi. Expression analyses were performed on fragments 20 days after amputation. In the real time RT-PCR experiment the expression level is indicated in relative units, assuming as unitary the value of the control. Samples were compared using the un-paired t-test. **P<0.001. The dashed yellow lines indicate the border between the regenerating area and the stump. Scale bar 200 μm.

Fig.7

Expression of *Djpiwi-1* after *Djmot* RNAi. A) Expression level analyzed by real time RT-PCR in water-injected (c) and in *Djmot* RNAi animals. **B-C)** Whole mount *in situ* hybridization in head fragments, 20 days after amputation. **B)** Water-injected control. **C)** A *Djmot* RNAi phenotype unable to regenerate, showing an indented wound region. The amputation level is represented by the yellow dashed line. **D)** A water-injected intact planarian. **E)** two *Djmot* RNAi phenotypes showing modification in the expression pattern near the posterior region of the brain. In real time RT-PCR experiment the expression levels are indicated in relative units, assuming as unitary the value of the control. Samples were compared using the un-paired t-test. *P<0.05. Scale bar 200 μm in B-C, 300 μm in D,E.

Fig. 8

Expression of *Djinx11, Djsyt and Djmhc-B* after *Djmot* RNAi, visualized by real time RT-PCR. A-C) expression level in water-injected (c) and in *Djmot* RNAi animals **A**) *Djinx11* **B)** *Djsyt* **C)** *Djmhc-B*. In real time RT-PCR experiments the expression levels are indicated in relative units, assuming as unitary the value of the control. Samples in (A) were compared using the un-paired t-test. *P<0.05.

Fig. 9

Hypothetical model for DjMot function in neoblasts. A) DjMot prevents nuclear translocation of p53–like protein**. B)** Phase contrast image of a neoblast. **C**) *Djmot*RNAi disrupts DjMot-p53 interaction and allows nuclear translocation of p53. **D**) Phase contrast image of a senescent cell, as detected after *Djmot*RNAi. Scale bar: 5μm.

Supplementary Fig.1

RNAi-mediated downregulation of *Djmot* in intact and regenerating animals, as visualized by real time RT-PCR. A) Expression level in water-injected (c: control) and *Djmot*RNAi intact animals. **B**) Expression level in water-injected (c: control) and *Djmot*RNAi planarians regenerating a tail. **C**) Expression level in water-injected (c: control) and *Djmot*RNAi planarians regenerating a head. In all experiments, the expression levels are indicated in relative units, assuming as unitary the value of water-injected controls. Each value is the mean ± standard deviation of 3 independent RNAi experiments, performed in triplicate.

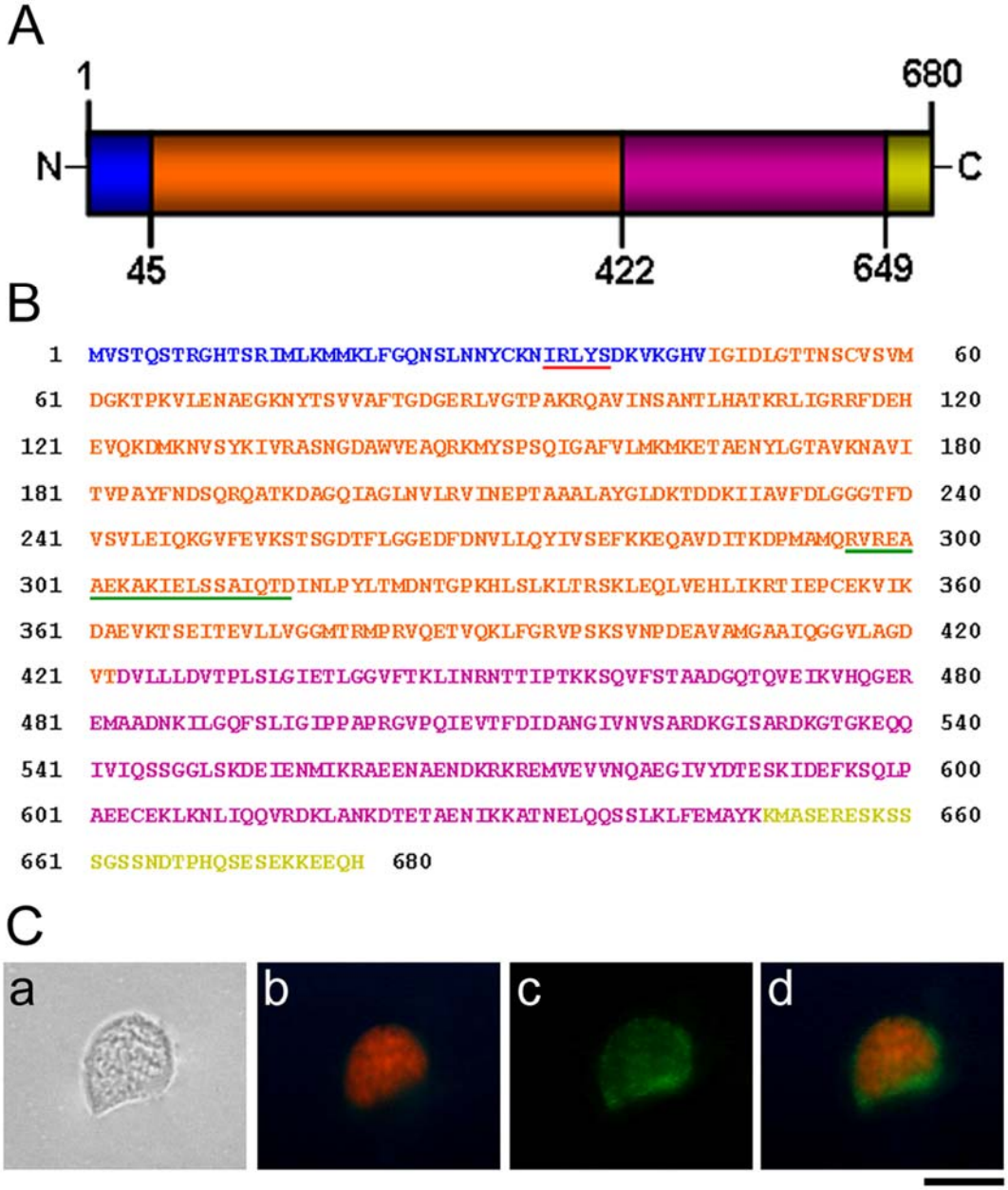

Fig.1: Djmot is a predicted orthologue of mammalian Mortalin. **A)** Schematic representation of Djmot protein and **B)** amino acid sequence deduced from the open reading frame of *Djmot* cDNA. Like other members of the Hsp70 family, Djmot is composed of two highly conserved regions: an amino-terminal ATPase domain (orange: amino acid 45-422) and a peptide binding domain (purple: amino acid 423-649). The sequence showing high similarity with the p53 binding region of *Mya arenaria* mortalin is underlined in green. The major differences with Mortalin proteins of other organisms are found in the first 44 residues of the N-terminal region (blue: presequence; the conserved mitocondrial localization signal IRLYS is underlined in red), and in the carboxy-terminal segment (yellow). In particular the C-terminal domain does not contain the conserved PTIEEVD motif, found in the constitutive form of HSP70 identified in *D. japonica* (DjHSC70: accession number ABY83101). **C)** Mamot antibody immunostaining on a dissociated neoblast-like cell **a)** Phase contrast image; **b)** Nucleus staining with ethidium homodimer (red). **c)** Expression of Mamot antibody (green). **d)** Merge of figures (c) and (d**)**. Scale bar 10 μm.

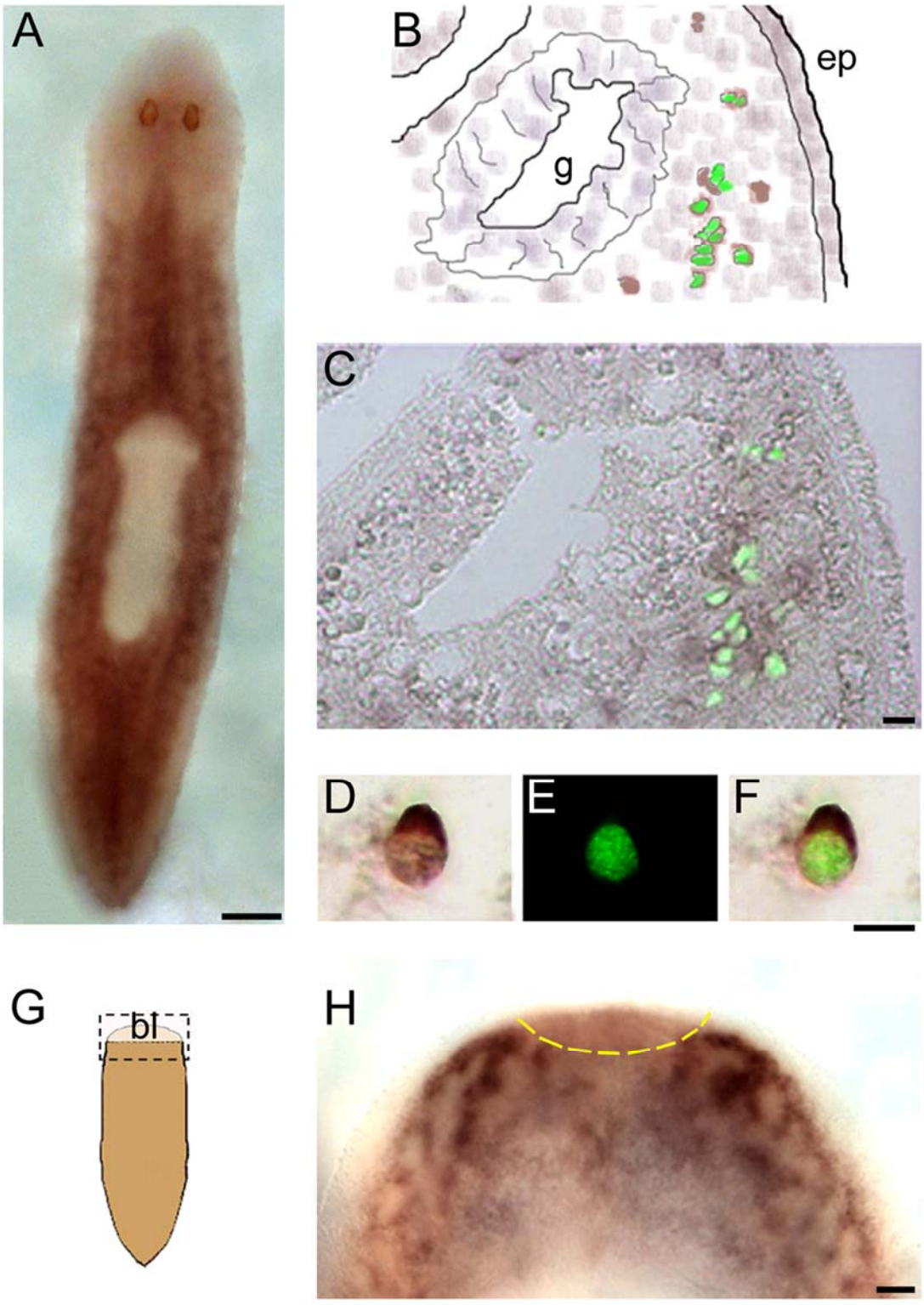

Fig.2: Analysis of *Djmot* expression in *D. japonica*. A) Whole mount *in situ* hybridization in an intact planarian. **B)** Schematic of the figure depicted in (C) (ep: epidermis; g: gut). **C)** *In situ* hybridization and DjPCNA antibody immunostaining on a transverse wax section: *Djmot* expression in purple and DjPCNA immunolocalization in green. **D)** Enlarged view of a neoblast-like cell expressing *Djmot* mRNA. **E)** The same cell after DjPCNA antibody immunostaining. **F)** Merge of D and E. **G)** Schematic of a planarian regenerating a head (bl: blastema). The region depicted in H is boxed. **H)** *Djmot* expression during head regeneration (2 days after amputation). The dashed yellow line indicates the border between the regenerating area and the stump. Anterior is on the top. Scale bars: 500 μm in A, 20 μm in C, 10 μm in D-F, 50 μm in H.

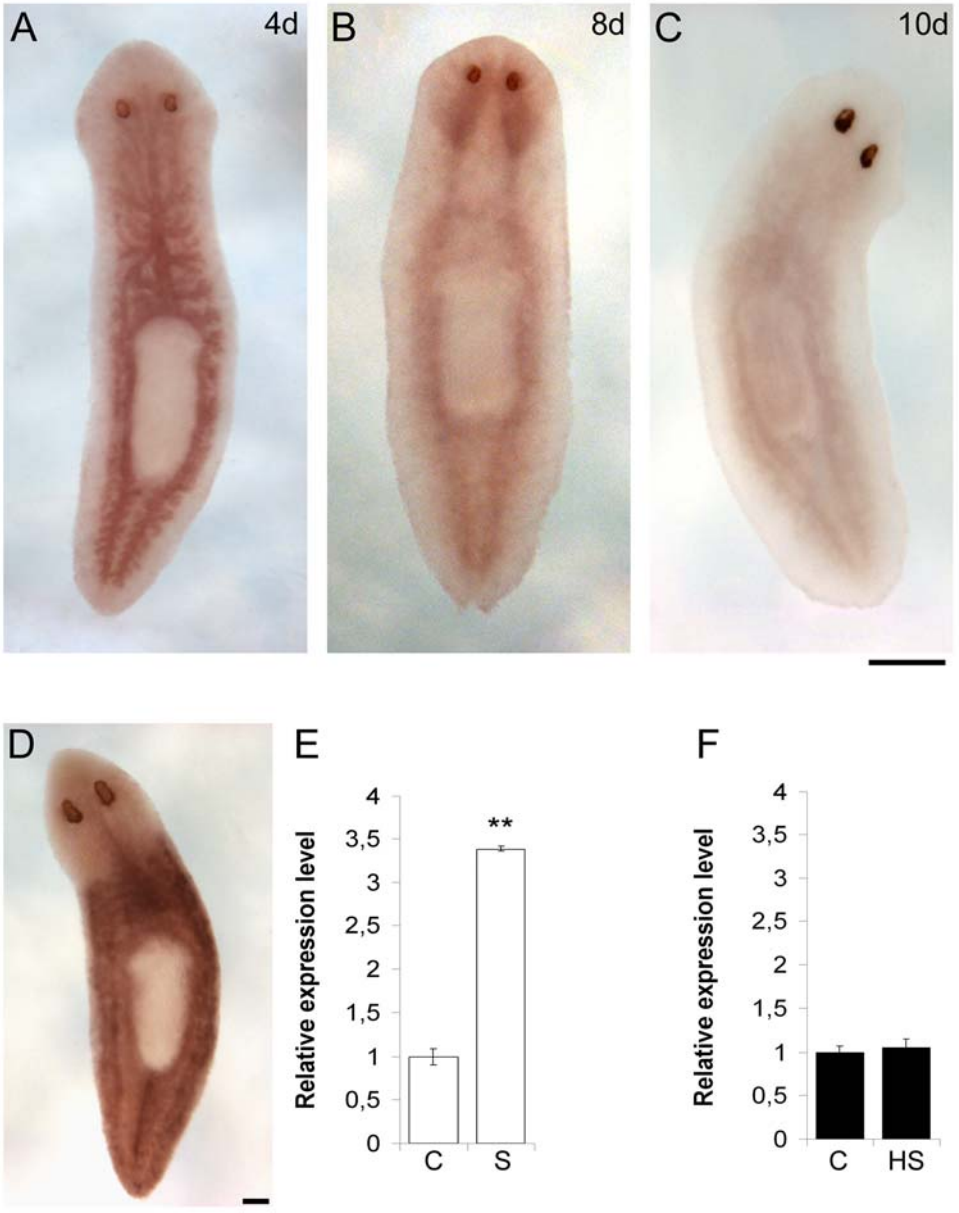

Fig.3 : ***Djmot* expression in different stress conditions**. **A-C)** Whole mount *in situ* hybridization analysis after X-ray irradiation (30Gy). **A**) 4d: 4 days after irradiation, **B**) 8d: 8 days after irradiation, **C**) 10d: 10 days after irradiation. **D,E)** *Djmot* expression analysis after starvation (30 days). **D**) Whole mount *in situ* hybrididazion. **E**) Real time RT-PCR. C: control, S: starved animals. Each value is the mean ± s.d. of three independent samples, analysed in triplicate. Samples were compared using the unpaired t-test.**P<0.001. **F)** Real time RT-PCR after heat shock (28°C for 20 hours) (C: control, HS heat shocked animals). Expression levels in E and F are indicated in relative units assuming as unitary the value of untreated specimens. Scale bars: 500 μm in A-C, 200 μm in D.

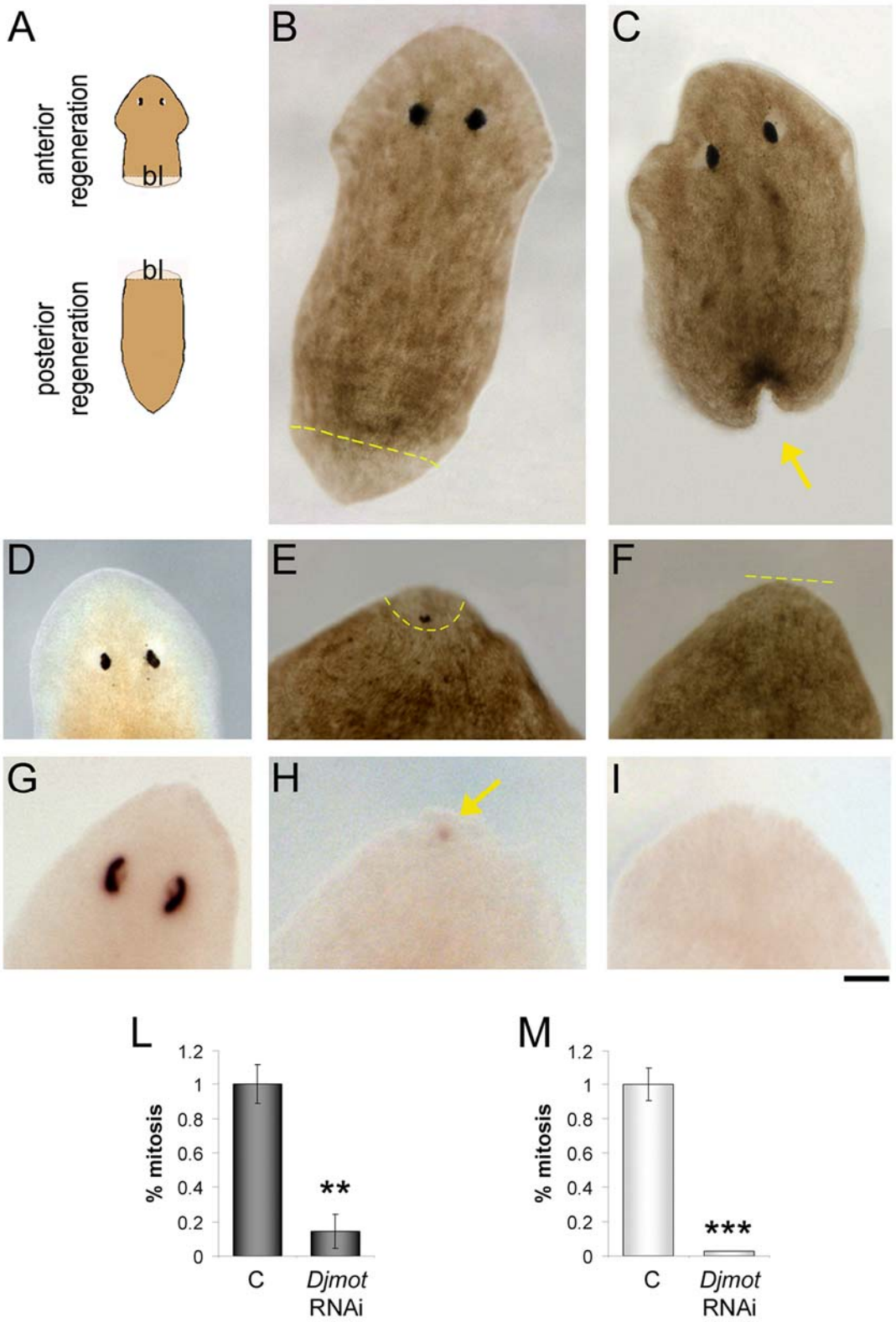

Fig.4: Analysis of *Djmot*RNAi phenotypes. A) Schematic of regenerating planarian fragments. bl: blastema. **B,C)** Bright-field images of head fragments, 20 days after amputation. **B)** A water-injected control regenerating a tail. The dashed yellow line indicates the border between the regenerating area and the stump. **C)** A *Djmot*RNAi phenotype. The wound region appears indented and does not form blastema (arrow). **D-F)** Bright-field images of tail fragments, 20 days after amputation. **D)** Visualization of a regenerated head of a water-injected control. **E)** A small, abnormal head is regenerated after *Djmot* RNAi. **F**) A phenotype unable to regenerate after *Djmot* RNAi. The dashed yellow line indicates the border between the regenerating area and

the stump. Anterior is on the top. **G-I)** Whole mount *in situ* hybridization with *Djops* of the planarian fragments depicted in D-F. **G)** *Djops* hybridization signal is clearly detected at the eye level in the water-injected control. **H)** *Djops* expression is detected in the small cyclopic eye of the small, abnormal head regenerated after *Djmot* RNAi. **I)** No *Djops* hybridization signal can be detected in the phenotype unable to regenerate after *Djmot* RNAi. **L)** Analysis of the percentage of mitoses in intact animals (dark gray) and **M**) during regeneration (light gray), (c: control). The number of mitotic metaphases was normalized to the number of total cells and the values indicated in the graphs are average ± s. d. of three independent samples. Samples were compared using the unpaired *t*-test. **P<0.001, ***P<0.0001. Scale bar 500 μm in B,C and 40μm in D-I.

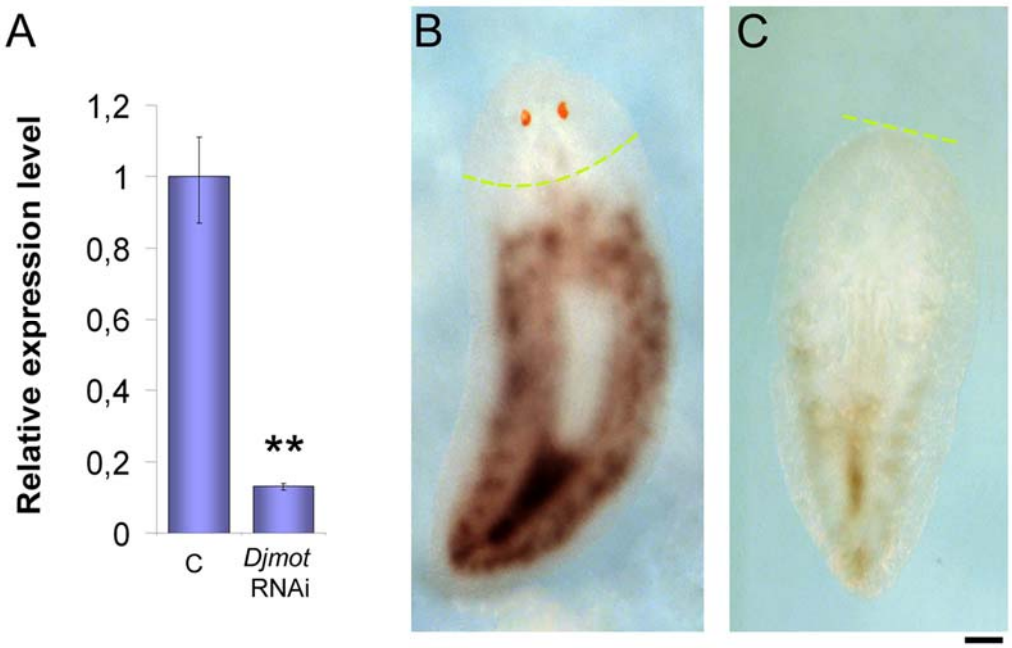

Fig.5 : Expression of *Djmcm2* after *Djmot* RNAi. A) Expression level analyzed by real time RT-PCR in water-injected controls (c) and in *Djmot* RNAi animals. **B)** Expression in a regenerating head of a water-injected control. **C)** Expression in a tail fragment unable to regenerate after *Djmot*RNAi. Expression analyses were performed on fragments 20 days after amputation. In the real time RT-PCR experiment the expression level is indicated in relative units, assuming as unitary the value of the control. Samples were compared using the un-paired t-test. **P<0.001. The dashed yellow lines indicate the border between the regenerating area and the stump. Anterior is on the top. Scale bar 200 μm.

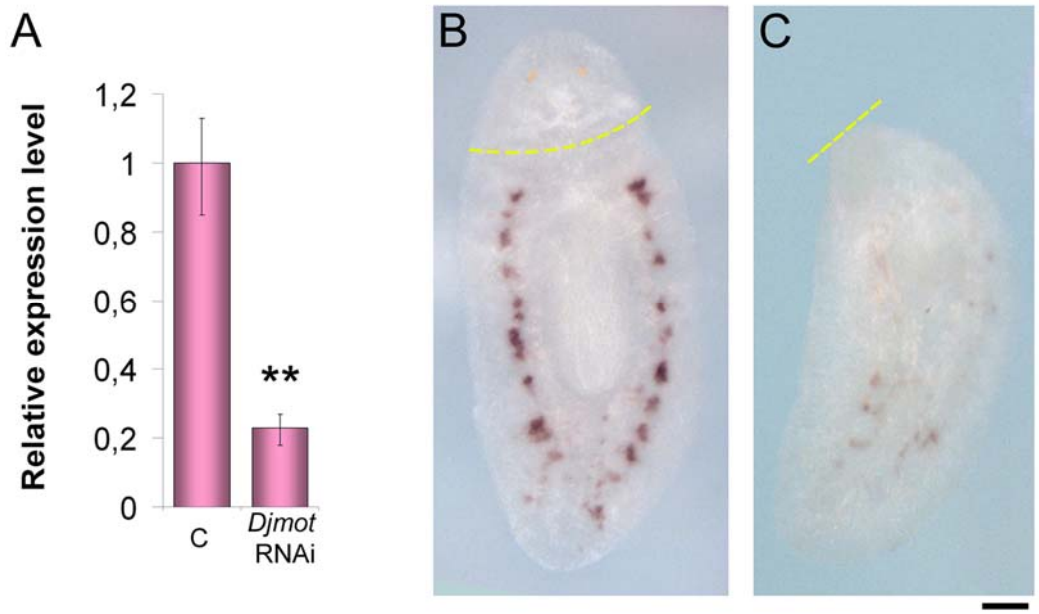

Fig.6 : Expression of *Djnos* after *Djmot* RNAi. A) Expression level analyzed by real time RT-PCR in water-injected controls (c) and in *Djmot* RNAi animals. **B)** Expression in a regenerating head of a water-injected control. **C)** Expression in a tail fragment unable to regenerate after *Djmot*RNAi. Expression analyses were performed on fragments 20 days after amputation. In the real time RT-PCR experiment the expression level is indicated in relative units, assuming as unitary the value of the control. Samples were compared using the un-paired t-test. **P<0.001. The dashed yellow lines indicate the border between the regenerating area and the stump. Scale bar 200 μm.

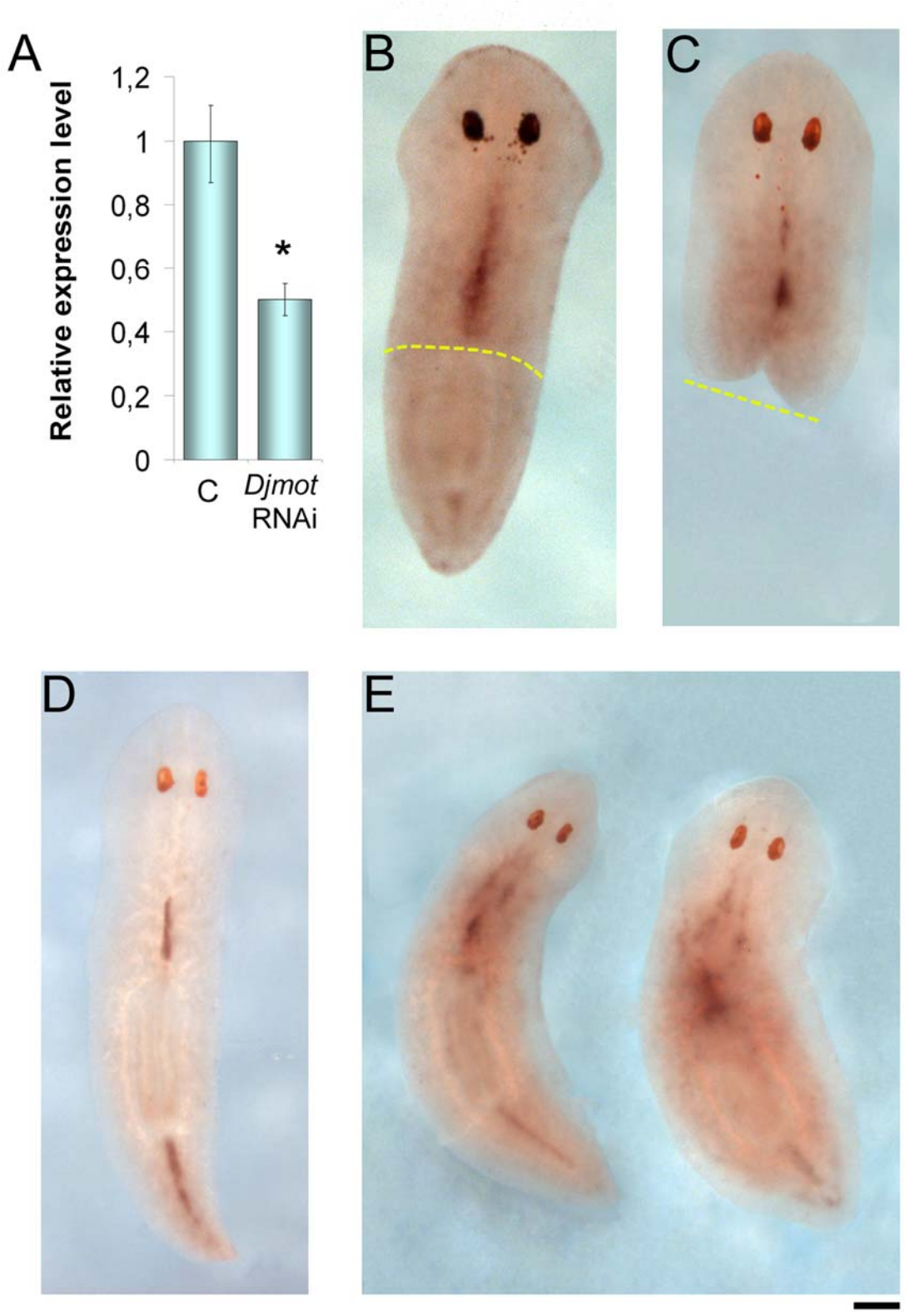

Fig.7 : **Expression of *Djpiwi-1* after *Djmot* RNAi. A)** Expression level analyzed by real time RT-PCR in water-injected (c) and in *Djmot* RNAi animals. **B-C)** Whole mount *in situ* hybridization in head fragments, 20 days after amputation. **B)** Water-injected control. **C)** A *Djmot* RNAi phenotype unable to regenerate, showing an indented wound region. The amputation level is represented by the yellow dashed line. **D)** A water-injected intact planarian. **E)** two *Djmot* RNAi phenotypes showing modification in the expression pattern near the posterior region of the brain. In real time RT-PCR experiment the expression levels are indicated in relative units, assuming as unitary the value of the control. Samples were compared using the un-paired t-test. *P<0.05. Scale bar 200 μm in B-C, 300 μm in D,E.

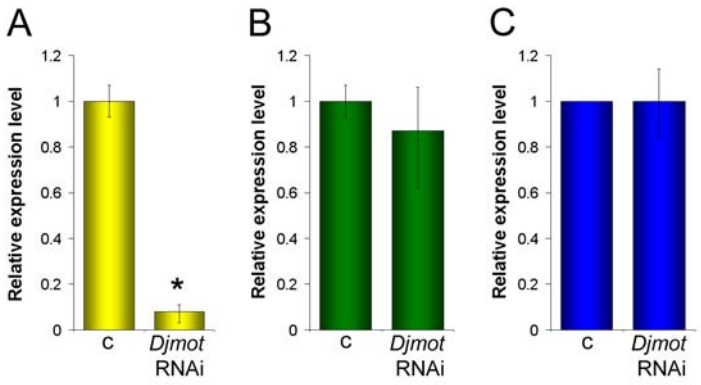

Fig.8 : Expression of *Djinx11, Djsyt and Djmhc-B* after *Djmot* RNAi, visualized by real time RT-PCR. A-C) Expression level in water-injected (c) and in *Djmot* RNAi animals **A**) *Djinx11* **B)** *Djsyt* **C)** *Djmhc-B.* In real time RT-PCR experiments the expression levels are indicated in relative units, assuming as unitary the value of the control. Samples in (A) were compared using the un-paired t-test. *P<0.05.

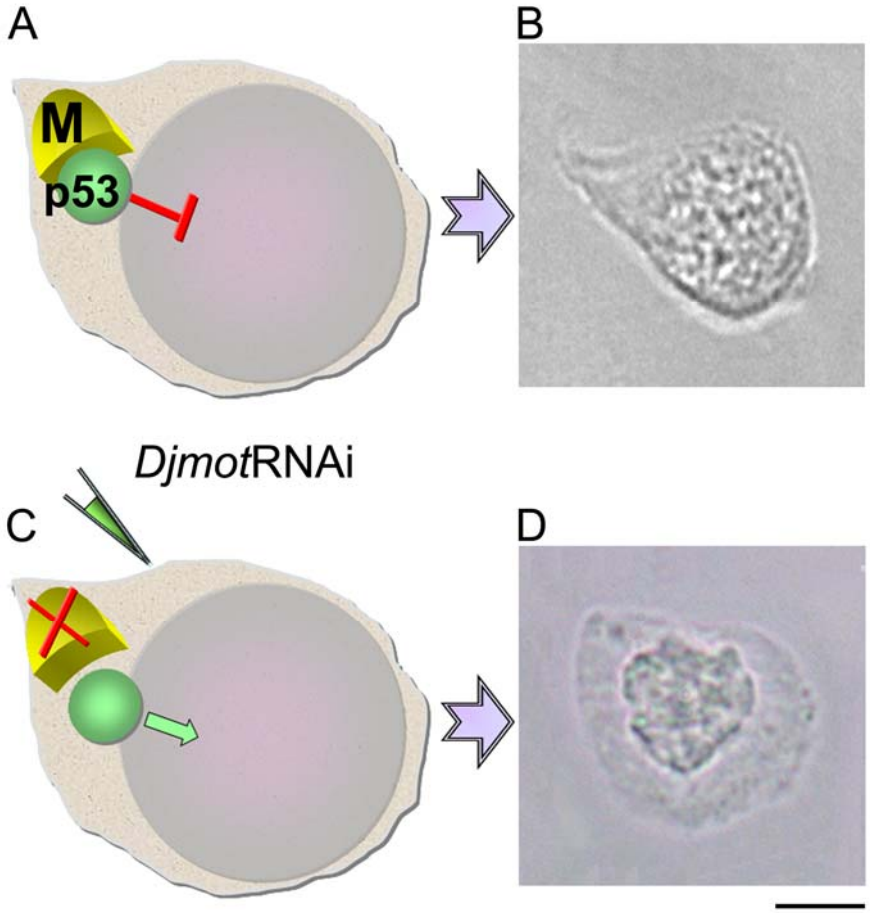

Fig.9 : Hypothetical model for DjMot function in neoblasts. A) DjMot prevents nuclear translocation of p53–like protein**. B)** Phase contrast image of a neoblast. **C**) *Djmot*RNAi disrupts DjMot-p53 interaction and allows nuclear translocation of p53. **D**) Phase contrast image of a senescent cell, as detected after *Djmot*RNAi. Scale bar: 5μm.

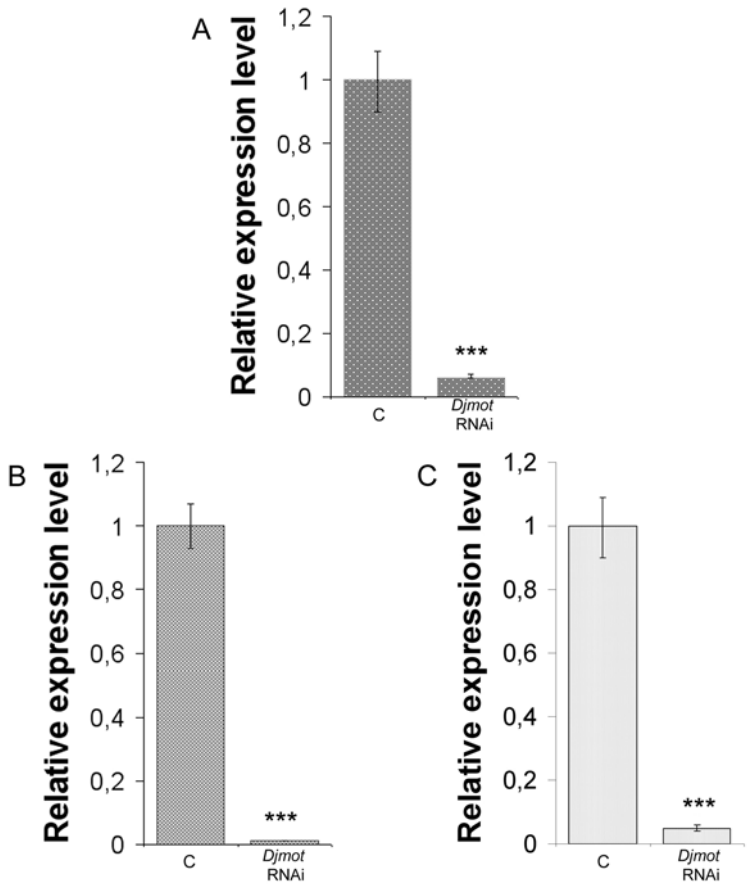

Suppl. Fig.1 : **RNAi-mediated downregulation of *Djmot* in intact and regenerating animals, as visualized by real time RT-PCR. A**) Expression level in water-injected (c: control) and *Djmot*RNAi intact animals. **B**) Expression level in water-injected (c: control) and *Djmot*RNAi planarians regenerating a tail. **C**) Expression level in water-injected (c: control) and *Djmot*RNAi planarians regenerating a head. In all experiments, the expression levels are indicated in relative units, assuming as unitary the value of water-injected controls. Each value is the mean ± standard deviation of 3 independent RNAi experiments, performed in triplicate.

Supplementary Table I.

Sense and antisense oligonucleotides used for real time RT-PCR

Gene name	Forward primer	Reverse primer
Djef2	5'-CAATCGAAGACGTTCCATGTG-3'	5'-AACACGAACAACAGGACTAACACT-3'
Djinx-11	5'-GTTGCTCAATGTGTGCTTCCTATC-3'	5'-GGTGGTTGACAACAAATAATATGAATC-3'
Djmhc-B	5'-CAACATCA TCAACGTGAATTGG-3'	5'-CCGTTGATAA ACTTAATGAGCT-3'
Djmcm2	5'-GATTACAGGCGAATTCCAGAACTT-3'	5'-GTCAGCCTGCGTTGTCGTC-3'
Djmot	5'-GCATTCCACCAGCACCTC-3'	5'-CATATTTTCAATTTCATCTTTACTCAA-3'
Djnos	5'-AGGAGTGATGTAAAATTATCCAAGG-3'	5'-GCTGACATACATTTCAAAAGGTTC-3'
Djpiwi-1	5'-GTTATGACGGACGACGACTATTTAC-3'	5'-CCTTTCCCTATTTTCTCTTGACC-3'
Djsyt	5'-TGGGAGCTATTGATTTGGGTC-3'	5'-ATGTGTATTTTTTTATCGTGGTCTTCT-3'